Available online at www.sciencedirect.com
ScienceDirect
Catalysis Today 125 (2007) 192–202
CATALYSIS TODAY
www.elsevier.com/locate/cattod

Deactivation patterns of Mo/Al_2O_3, $Ni–Mo/Al_2O_3$ and $Ni–MoP/Al_2O_3$ catalysts in atmospheric residue hydrodesulphurization

A. Marafi [a,*], A. Hauser [b], A. Stanislaus [a]

[a] *Petroleum Refining Department, Kuwait Institute for Scientific Research, P.O. Box 24885, 13109 Safat, Kuwait*
[b] *Central Analytical Laboratories, Kuwait Institute for Scientific Research, P.O. Box 24885, 13109 Safat, Kuwait*

Available online 7 May 2007

Abstract

In the present work, a comparative study on the deactivation behavior of three types of industrial hydrotreating catalysts, namely, Mo/Al_2O_3, $Ni–Mo/Al_2O_3$ and $Ni–MoP/Al_2O_3$, that are used to promote primarily hydrodemetallization (HDM), hydrodesulphurization (HDS) and hydrodesulphurization + hydrodenitrogenation (HDS/HDN) reactions, respectively, in the first, second and third reactor of commercial atmospheric residue desulfurization (ARDS) units was carried out. The main objective of the study was to contribute to a better understanding of the relationship between catalyst type and catalyst deactivation patterns. The used catalysts from these experiments were fully characterized to determine the extent and the cause of deactivation. Special emphasis was paid to understanding the nature of the coke and metal deposition on the used catalysts by applying chemical analysis and various advanced analytical techniques, such as solid-state carbon-13 nuclear magnetic resonance spectroscopy (^{13}C NMR), temperature-programmed oxidation (TPO), electron probe micro-analysis (EPMA), and diffuse reflectance infrared Fourier transform (DRIFT) spectroscopy. The results are discussed scientifically based on the physico–chemical properties of the three catalysts.

Keywords: ARDS process; Heavy oil upgrading; Coke formation; Deactivation by metal and coke

1. Introduction

The atmospheric residue desulfurization (ARDS) process is extensively used in Kuwait's refineries for upgrading residues [1–3]. The process involves hydrotreatment of atmospheric residue in a series of fixed bed reactors containing catalysts. The ARDS process unit works primarily as a desulfurization unit, but also reduces the metals, asphaltenes, and nitrogen in the products, thereby, ensuring proper quality of purified feed for downstream conversion units (i.e., fluid catalytic cracking (FCC) and delayed coker). As an additional benefit, mild hydrocracking also occurs in the ARDS process with the conversion of residues to distillates, like naphtha, kerosene and diesel.In ARDS, graded catalyst systems in multiple reactors are used in order to achieve hydrodemetallation (HDM), hydrodesufurization (HDS), hydrodenitrogenation (HDN), and conversion of residues to distillates at desired levels. Three types of catalysts, namely, a HDM catalyst for metal removal in the front reactors, a HDM/HDS catalyst with balanced HDM and HDS activities in the middle section and a very active HDS/HDN catalyst in the last reactor, are commonly used in the ARDS process. The performance of the ARDS process regarding the degree of HDM, HDS, HDN reactions, conversion to distillates and life-on-stream is closely linked to the catalyst system [4,5]. The catalytic materials used in the process are almost exclusively based on sulfides of molybdenum with cobalt or nickel as promoters that are supported on an alumina carrier. During the hydrotreating process, the catalysts deactivate by the deposition of coke and metals [6–9]. Coke deposition on residual oil hydrotreating catalysts is more extensive during the early stages of operation. Initial coking is reported to cause a large loss in surface area and a fairly rapid deactivation of the catalyst. Three stages of catalyst deactivation, namely, a rapid initial deactivation by coke deposition, a steady-state gradual deactivation in the middle of the run and a very rapid final deactivation at the end of the run by pore mouth plugging have been identified in residual ARDS operation [10].

* Corresponding author. Tel.: +965 3980499; fax: +965 3980445.
E-mail address: amarafie@prsc.kisr.edu.kw (A. Marafi).

0920-5861/$ – see front matter
doi:10.1016/j.cattod.2007.03.060

The catalysts used in the process play a major role in accomplishing the process objectives with respect to various conversions and run length. Each one of these catalysts has different properties which may influence their deactivation during the operation, differently. A clear understanding of the deactivation behavior of the individual catalysts is important and highly desirable to optimize the reactor loading as well to prolong on-stream efficiency which improves the overall process economics.

In the present work which is a continuation of our studies on catalyst deactivation in the ARDS process [11–14], a comparative study on the deactivation behavior of three types of industrial hydrotreating catalysts, namely, Mo/Al_2O_3 (HDM), $Ni–Mo/Al_2O_3$ (HDS) and $Ni–MoP/Al_2O_3$ (HDS/HDN), used in the first, second and third reactor of commercial atmospheric residue desulfurization (ARDS) units was carried out. Although, in an industrial unit, these three tested catalysts are exposed to different feeds, the experiments were conducted with the same feedstock, Kuwait atmospheric residue (KAR), to make the results comparable. The primary objective of the study was to contribute to a better understanding of the relationship between catalyst type and catalyst deactivation patterns during the initial stage of the ARDS process. The extent of deactivation by coke formation and nature of the carbonaceous deposit on the three types of catalysts as well as the extent of metal deposition on different catalysts and their deactivation role were also examined. Special emphasis was paid to understanding the nature of the coke and metal deposition on the used catalysts by applying chemical analysis and various advanced analytical techniques, such as solid-state ^{13}C NMR, TPO, EPMA, and IR.

2. Experimental

2.1. Materials

Catalysts. Three types of industrial catalysts, namely, Mo/Al_2O_3 (low metal content), $Ni–Mo/Al_2O_3$ (medium metal content), and $Ni–MoP/Al_2O_3$ (high metal content), further denoted as CAT A, CAT B, and CAT C, respectively, were tested in the hydrotreating experiments. The same catalysts are used by Kuwait National Petroleum Company (KNPC) refinery in one of its ARDS units. The characteristics of the catalysts are presented in Table 1.

Feed. The feed (KAR) used in the tests is essentially the same residue which is hydrotreated in the KNPC's ARDS unit. The feedstock's main characteristics were determined and are presented in Table 2. The experimental details and the equipment used for feedstock characterization by various techniques were the same as reported in our previous papers [12,14].

2.2. Pilot plant hydrotreating tests

Catalyst performance test was conducted using a fixed bed single micro-reactor testing unit. 30 ml of catalyst was diluted with equal amount of carborundum and loaded at the center of the reactor; the feed flow direction was down-flow mode. The catalyst was presulfided using 1% CS_2 in the straight run gas oil by the standard procedure [13] before introducing the feed. After presulfiding the test conditions are adujested to the desired operating conditions. The operating conditions employed for all experiments are presented in Table 3.

Table 1
Physical properties of fresh HDM, HDS and HDS/HDN catalysts used in the study

Physical property	Unit	Catalyst		
		CAT A	CAT B	CAT C
Bulk density	g/ml	0.4–0.6	0.6–0.8	0.7–0.8
Surface area	m^2/g	150–200	200–250	170–200
Pore diameter		Large	Medium	Small
Average metal content		Low	Medium	High

2.3. Catalyst characterization

The used catalysts were collected from various hydrotreating experiments and cleaned using toluene extraction in a soxhlet apparatus till the toluene extract was clear (free from oil) before subjecting them to characterization by different techniques, such as surface area and pore volume measurement, chemical analysis, elemental (C, H, S, N) analysis, EPMA, TPO, ^{13}C NMR spectroscopy and DRIFT spectroscopy. The equipment and the procedures used for these tests are described in detail in our previous papers [11,12,14].

3. Results and discussion

In the ARDS process, catalysts play an important role. The process performance with regard to various conversions and run length is linked to activity, selectivity and deactivation behavior of the catalysts used in the process. In the present study, hydrotreatment of KAR was separately carried out over three types of commercial ARDS catalysts to evaluate the relation between catalyst properties and deactivation behavior. The operational conditions were: reactor temperature 380 °C, LHSV 1 h^{-1} and time-on-stream (TOS) 120 h. The used catalysts were fully characterized by various techniques.

With regard to the used catalysts, the deposits are described in terms of coke deposition which comprises the elements carbon, hydrogen, sulfur and nitrogen, as well as moisture and metal deposits. The deposits are then further characterized by quantification of groups of constituents, e.g., metal sulfides, soft and refractory coke. The coke is investigated in more detail by solid-state ^{13}C NMR to elucidate its average structure. Additionally, alterations in the catalyst's physical properties, such as surface area, pore volume and average pore diameter, due to coking and metal deposition are reported. The analysis results are reported with emphasis on:

1. the chemical composition of the deposits;
2. the types of carbonaceous deposits;
3. the average structural features of the coke;

Table 2
Characteristics of the Kuwait atmospheric residue (KAR), maltene fraction and asphaltene fraction

Property	Unit	Feedstock		
		KAR	Maltene	Asphaltene
Content	wt.%	100	96.4	3.6
Density at 15 °C	g/ml	0.9837		
Density at 65 °C	g/ml	0.9507		
API gravity	–	12.27		
Kinematic viscosity at 50 °C	cSt	871.2		
Asphaltenes	wt.%	3.6		
Conradson carbon residue (CCR)	wt.%	12.20		
Carbon content	wt.%	83.4	83.4	77.2
Hydrogen content	wt.%	11.4	11.1	7.1
Sulfur content	wt.%	4.3	4.2	8.8
Nitrogen content	wt.%	0.29	0.2	0.9
Total metals content	ppm	97	8	2286
V content	ppm	69	4	1810
Ni content	ppm	21	4	476
Na content	ppm	2		
Fe content	ppm	5		
Average structural parameters[a]				
Carbon in saturated building blocks[b]	wt.%	74.6	75.5	49.6
Carbon in n-alkanes[b]	wt.%	35.4	35.9	21.4
Carbon in CH_3 -group[b]	wt.%	10.6	10.7	6.9
Carbon in aromatic building blocks[b]	wt.%	25.4	24.5	50.4
Tertiary aromatic carbon[b]	wt.%	8.8	8.5	17.1
Alkyl-substituted aromatic carbon[2]	wt.%	17.6	17.8	12.3
Quaternary aromatic carbon[b]	wt.%	16.6	16.0	33.3
Aromaiticity (fa)[b]		0.25	0.24	0.50
Degree of substitution (σ)[b]		0.40	0.40	0.32
Degree of condensation (γ)[b]		0.18	0.17	0.57

[a] Normalized to 100% carbon.
[b] For calculation see text.

4. the distribution of deposited metals on the catalyst pellets;
5. changes in surface area, pore volume and pore size.

3.1. Coke deposition

Table 4 compares the chemical composition of the carbonaceous deposits found on the three types of industrial ARDS catalysts that are designed for specific process objectives, namely, HDM (CAT A), HDS (CAT B) and HDS/HDN (CAT C). The data correspond to 100 g of fresh catalyst without moisture.

Generally, the coking tendency of all three catalysts is quite high. Nevertheless, there are certain differences in the amount of carbon accumulation that increases in the following sequence:

$$\text{CAT B (HDS)} < \text{CAT A (HDM)} < \text{CAT C (HDS/HDN)}$$

Table 3
Operating conditions of hydrotresting experiments

Process parameter	Condition
Temperature (°C)	380
Pressure (bar)	120
LHSV (h^{-1})	1.0
H_2/Oil ratio (ml/ml)	680
Time-on-stream (h)	120

The reason for the differences in the coking tendency of the three catalysts is not clear. Coke formation on a hydrotreating catalyst is usually influenced by several factors, such as feedstock type, operating conditions and properties of the catalyst. If the feedstock and operating conditions are not varied, the differences in the coking propensity of different catalysts could be attributed to the differences in the properties of the catalysts. Catalyst type, acidity, pore size distribution and hydrogenation function are important parameters that play a major role on coke deposition on the catalyst during hydrotreating operations. Generally, the rate and extent of coke formation increase with concentration and strength of acid sites in the catalyst. Catalysts with high hydrogenation activity usually reduce the extent of coke formation by removing the

Table 4
Chemical composition of the carbonaceous deposit on three industrial, ARDS catalysts exposed to KAR for 120 h at 380 °C and LHSV 1 h^{-1}

Parameter	ARDS catalyst		
	CAT A	CAT B	CAT C
Carbon (wt.%)	21.17	18.8	22.72
Hydrogen (wt.%)	2.15	2.01	2.21
Sulfur (wt.%)	2.54	7.25	9.49
Nitrogen (wt.%)	0.38	0.39	0.54
H/C ratio	1.22	1.28	1.17

coke precursors adsorbed on the catalyst surface by hydrogenation. The extent of coke deposition has been found to decrease with increasing pore size.

The three types of catalysts used in the present work had different properties. CAT A contained unpromoted MoO_3 on ϒ-alumina support. The catalyst also had wider pores than the others. CAT B contained both Ni and Mo, and had pores having an average diameter smaller than that of CAT A and larger than that of CAT C. CAT C contained higher concentrations of Mo and Ni than those of CAT B, together with phosphorus. The acidity of the catalyst usually depends on the type of support used and on the metal contents. The differences between the three catalysts in key properties, namely, metal contents, hydrogenation function, pore size and acidity, can be summarized as follows:

Catalyst property	Ranking
Active metal content	CAT C (HDS/HDN) > CAT B (HDS) > CAT A (HDM)
Hydrogenation function	CAT C (HDS/HDN) > CAT B (HDS) > CAT A (HDM)
Pore size	CAT A (HDM > CAT B (HDS) > CAT C (HDS/HDN)
Acidity	CAT C (HDS/HDN) > CAT B (HDS) > CAT A (HDM)

The higher coke formation on CAT A compared with that of CAT B can be attributed to its lower hydrogenation function. The deposition of more coke on CAT C than on CAT B is, however, not consistent with its higher hydrogenation activity. This is probably due to the difference in the acid function of the catalysts. Catalysts used in the back-end reactors, such as CAT C, are usually designed with a higher acidity and hydrogenation function than the others to promote HDN and hydrocracking (HC) reactions. It appears that the acid function plays a more dominating role than the hydrogenation function of catalyst C. The acidity of the catalyst is mainly associated with the support. The HDS/HDN catalyst (CAT C) used in the present study was $NiMoP/Al_2O_3$. Although, phosphorus modifies the acidity of the γ-Al_2O_3 support, it does not increase the acid strength [15]. It is likely the alumina support used in CAT C is specially designed with higher acidity or mixed with some acidity enhancing components (e.g. zeolite). The higher the acidity is, the more cracking takes place and more coke is formed. The coke precursors will be usually removed by hydrogenation. In addition, the smaller pore size of the catalyst C could also have contributed to coke formation [16]. Poisoning of the hydrogenation sites by adsorption of nitrogen compounds and NH_3 and H_2S from the gas stream may suppress the hydrogenation function to some extent. The higher nitrogen content of the coke deposit on this catalyst is consistent with this.

The sulfure content of the three catalysts is clearly different and increases in the following sequence:CAT A (HDM) > CAT B (HDS) > CAT C (HDS/HDN)

Hydrotreating catalysts need to be sulfided before they are used in an ARDS process. Consequently, there are two sources of sulfur on used catalysts: sulfur in the active catalyst metal sulfides and sulfur in deposits. The deposits consist predominantly of coke and metal sulfides generated from the feed species. The elemental analysis only provides the total sulfur on the used catalyst, therefore, this value provides limited information with regard to deactivation. Nevertheless, since sulfur is strongly associated with the metals, the catalyst with the highest metal content shows the highest sulfur content. A differentiation between both types of deposited sulfur, sulfur in coke and sulfur as metalsulfide can be obtained by TPO-MS. This point is discussed in the following section.

3.2. Coke type

Coke deposits on the catalyst occurring during hydrodesulfurization of residua have been classified into three types [17]:

1. Reversibly adsorbed aromatics;
2. Reversibly adsorbed asphaltenes;
3. Irreversibly adsorbed highly condensed aromatic clusters.

The first two types of coke are also classified as soft or bulk coke which is characterized by a high H/C ratio and solubility in organic solvents like toluene or THF. For example, it was found that sludge produced during catalytic hydrocracking of vacuum residue from Arabian light oil (bp > 550 °C) was soluble in hexane, benzene and THF to 86%, 7% and 2%, respectively [18]. Depending on the period of coking, the completely insoluble fraction of coke is usually classified as refractory surface or hard coke, and the latter possesses a remarkably low H/C ratio.

In the case of metal sulfides supported on alumina, both kinds of coke are formed: high (H/C) ratio coke on the metal sites (hydrogenation or hydrogenolysis sites), and low (H/C) ratio coke on the alumina support which contains acidic cracking and condensation sites [19]. The results presented in Table 4 shows that the H/C ratio of deposited coke on the three types of catalysts are well above 0.6, usually found for aged coke deposits [12]. The initial coke that is rich in hydrogen undergoes dehydrodegenation and condensation reactions to increase hard coke with increasing catalyst age.

3.2.1. TPO-MS

To study the combustion behavior of the carbonaceous deposit on a used catalyst which allows a classification of coke components, the TPO-MS technique is the method of choice [11,20–22]. In Figs. 1–4, the formation of the major gaseous combustion products, namely, CO_2, SO_2 and NO_2, versus temperature is displayed for the three types of used catalysts, HDM, HDS, HDS/HDN, respectively. The graphs indicate that there were two distinct combustion intervals for carbon and the heteroatoms nitrogen and sulfur were oxidized in the temperature ranges from 150 °C to 350 °C and from 350 °C to 550 °C. Carbon burned off from 250 °C up to 550 °C, where the peak showed a shoulder towards the low temperature side of the axis, but the shoulder appeared at a higher temperature (ca. 325 °C) than the low temperature SO_2 and NO_2 peak (ca. 265 °C) did.

Regarding the deposited carbon, the combustion went through two stages, one at about 325 °C and another one at

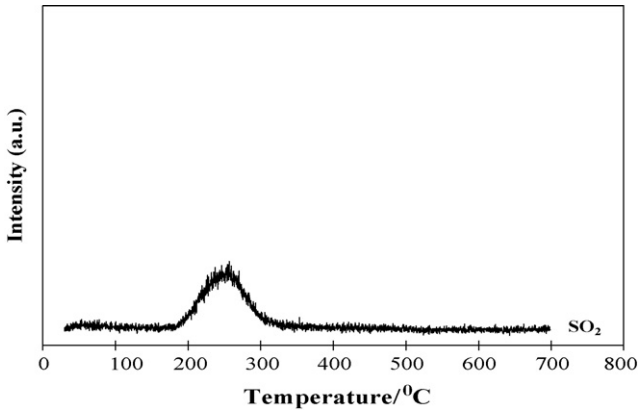

Fig. 1. SO_2 profile for TPO of fresh CAT A after presulfiding.

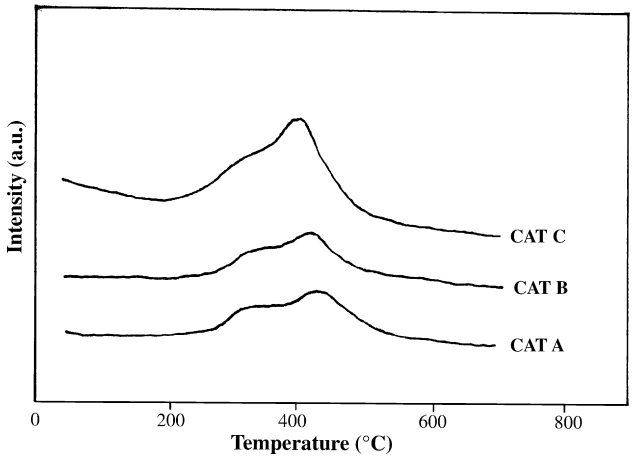

Fig. 2. CO_2 profile for TPO of used CAT A, CAT B and CAT C.

about 400 °C indicating, the presence of two types of coke. The two fractions of coke were classified as soft coke which can be removed more easily, and as refractory surface coke which is more difficult to remove. The refractory coke is strongly adhered to the surface of the support [23–25]. The soft coke, on the other hand, is a porous and bulky material that is rich in

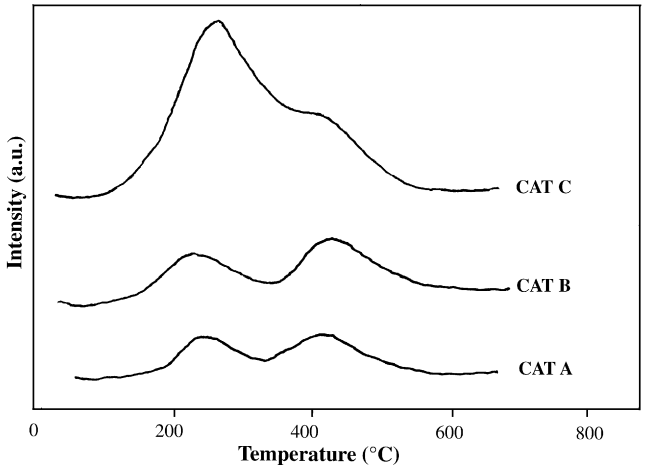

Fig. 3. SO_2 profile for TPO of used CAT A, CAT B and CAT C.

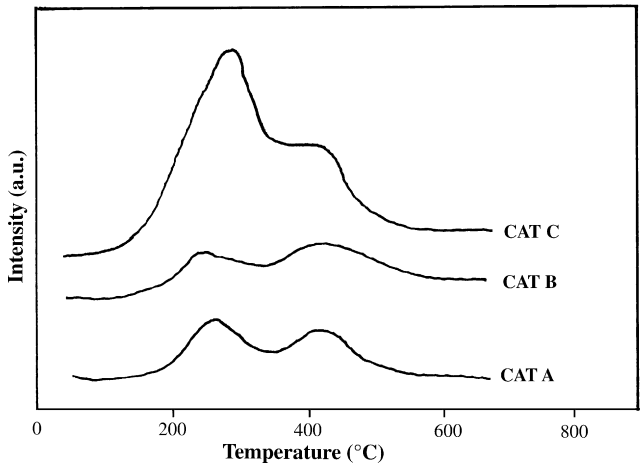

Fig. 4. NO_2 profile for TPO of used CAT A, CAT B and CAT C.

hydrogen and represents an intermediate phase between coke precursors from the feed and coke. During initial coking, both types are formed.

Although, there is a certain overlapping of the two CO_2-peaks, curve deconvolution allowed a semi-quantitative estimation of the coke types formed during initial coking. As presented in Table 5, the ratio between the two types varied and was correlated with the available surface area of the fresh catalysts in the reactor.

In the case of NO_2 and SO_2, the first peaks appeared even before the formation of CO_2 started. The SO_2 peak at around 265 °C was suggested to originate from the oxidation of inorganic sulfur associated with the metals in the catalyst (e.g., MoS_2, NiS) [26]. Yoshimura et al. [27] reported the formation of a single SO_2 peak at about 260 °C during the TPO MoS_2/Al_2O_3. This was further confirmed by temperature-programmed oxidation of an only presulfided HDM catalyst ($MoO_3/A1_2O_3$) that generated merely one peak which appeared at the same temperature as the low temperature SO_2 peak did, without any indication of a high temperature peak (Fig. 1). Sulfided Ni in used Ni–Mo/Al_2O_3 catalyst may be present in more than one form such as NiS, Ni_2S_3. SO_2 formation during the TPO presulfided NiO/Al_2O_3 catalyst has been reported to occur in a wide temperature range 180–280 °C overlapping with the SO_2 peak formed from MoS_2 oxidation. The fact that the low temperature NO_2 and SO_2 peaks coincided proves that a part of the nitrogen is associated with the metal sulfide sites in the catalyst. This observation suggests an initial poisoning mechanism, in which some nitrogen compounds were strongly

Table 5
Ratio of surface to soft coke on used ARDS catalysts and surface area of fresh catalysts

Catalyst	Surface coke[a] (%)	Soft coke[a] (%)	Ratio surface/soft coke	Surface area[b] (%)
CAT A	78.9	21.1	3.74	100
CAT B	88.1	11.9	7.40	163
CAT C	84.4	15.6	5.41	134

[a] Normalized to 100%.
[b] Available surface area normalized to 100% for fresh catalyst A.

adsorbed at the active metal phase as soon as the feed was introduced [6,11,21,28,29]. This also implies that, during the initial phase of coking, the active metal sulfide phase started to deactivate rather by poisoning than by carbon fouling. As observed for the low temperature SO_2 peak (Fig. 3), the intensity of the low temperature NO_2 peak also correlated with the amount of metal found on the used catalysts which confirms the association of nitrogen with the active metal sulfide phase (Fig. 4).

The absence of any CO_2 peak coinciding with the low temperature NO_2 and SO_2 peaks (Figs. 3 and 4) which resulted from oxidation of nitrogen and sulfur associated with the metals on the used catalysts, clearly showed that, during the initial phase of coking, no carbon was deposited on the active metal sulfide phase. It is likely that the initial coke was deposited on the support surface, but not at the active metal sulfide phase. This observation confirms the model of initial coking suggested by [30,31].

Another remarkable fact is that N and S were mainly concentrated either in the hard coke or at the metal, but scarcely in the soft coke which confirms the hypothesis that, in the early stages of coking, hetero-compounds are embedded in the surface coke or adsorbed at the metal crystallites.

In summary, the TPO-MS studies confirm our earlier conclusions on the nature of initial coke, i.e.: (i) two types of coke, soft and hard (or refractory) are deposited on the catalyst; (ii) the active metal sulfide phase is not covered with initial coke; (iii) heteroatoms, such as nitrogen and sulfur, are present in the hard (surface) coke, but not in the soft coke; and (iv) during the initial stage of coking, the active metal sulfide phase starts to deactivate rather by poisoning than by carbon fouling. In addition, the studies show that nitrogen poisoning is more severe on the back-end catalyst (C) that contains a higher active metal content than the front-end HDM catalyst (A), containing a low concentration of unpromoted MoO_3. The ratio between the two types of coke formed on different catalysts is strongly influenced by the strength of their acidic and hydrogenation functions.

3.3. Coke structure

Solid-state ^{13}C NMR. The structural characterization of carbonaceous deposits on used catalysts is based on the fact that the deposited hydrocarbons are formed of a limited number of building blocks (Fig. 5 and Table 6).

These building blocks give rise to ^{13}C NMR resonances within specific chemical shift ranges. Integration over these chemical shift ranges allows a quantification of the building blocks in the coke structure. The error of the integration amounts up to 3% of the integral value.

Paramagnetic species, like graphite or metals, embedded in the coke interact with the ^{13}C nuclei, resulting in extremely broadened NMR peaks, making them invisible to NMR. To estimate the amount of NMR invisible carbon, the used CAT A was selected. The sample was mixed with a known amount of glycine and the SEP/MAS ^{13}C NMR spectrum was measured. Both values, wt.% of NMR visible carbon (C_{NMR}) and wt.% carbon found by elemental analysis (C_{EA}), differed only by 0.4 wt.% (Table 7), indicating that there is not much graphite built at that stage of coking and the effect of paramagnetic metals, for instance, vanadium and nickel, is negligible.

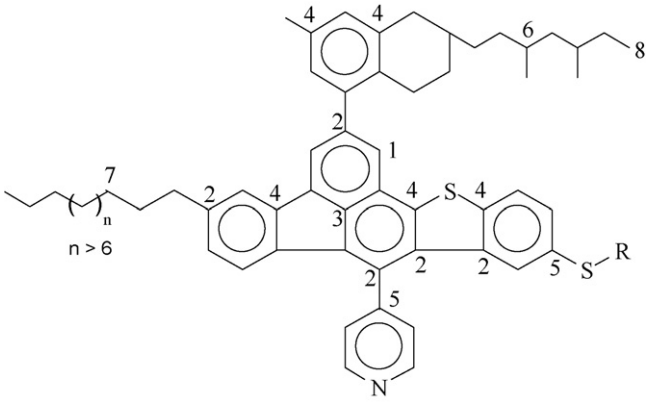

Fig. 5. Hypothetical structure of a coke deposit.

Table 6
Carbon building blocks in coke

Number	Building block[a]	Type	Class	Symbol
1	CCCH	Aromatic	Tertiary	wt.% Car; t
2	CCC	Aromatic	Quaternary	wt.% Car; alk
3	CCC	Aromatic	Quaternary	wt.% Car; b3
4	CCC	Aromatic	Quaternary	wt.% Car; b2,n, CH3
5	CCCN, CCCS	Aromatic	Quaternary	wt.% Car; x
6	CCCH	Aliphatic	Tertiary	wt.% Cal; t
7	CCHH	Aliphatic	Secondary	wt.% Cal; s
8	CHHH	Aliphatic	Primary	wt.% Cal; p

[a] See Fig. 5.

The most prominent structural parameter in characterizing carbonaceous deposits formed by conversion of hydrocarbons on catalysts is the ratio of aromatic to total carbon on the used catalyst which refers to the aromaticity of the deposit. The value varies between zero, totally aliphatic (paraffinic), and one, totally aromatic (graphitic), and the closer the value reach to one, the more condensed and aromatic hydrocarbons are deposited. On the one hand, severe reaction conditions, such as high temperature, long TOS and low LHSV, increase both decomposition and condensation of hydrocarbons, leading to a highly aromatic carbon deposit. On the other hand, the lesser the hydrogenation activity and the higher the cracking activity of the catalyst, the more coke is formed.

Principally, coke formation on ARDS catalysts is a result of adsorption, dehydrogenation, cracking and condensation

Table 7
Determination of NMR visible carbon (wt.% C_{NMR}) on used CAT A (HDM)

Sample	CAT A
C_{EA} (wt.%)	17.3
C_{NMR} (wt.%)	16.9
Diff. (wt.%)	−0.4

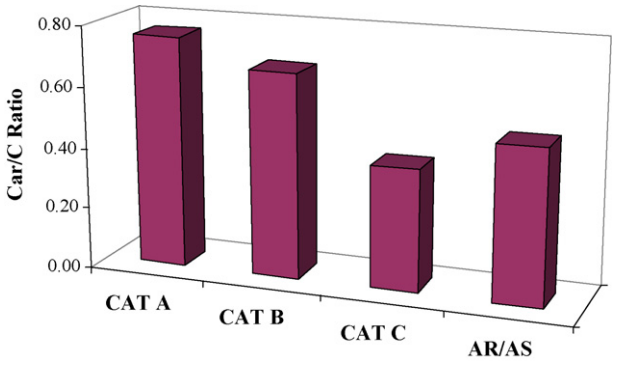

Fig. 6. Ratio of aromatic to total carbon in coke on the used catalysts A, B and C.

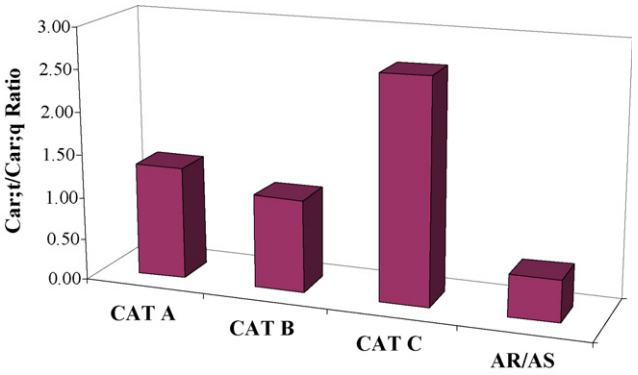

Fig. 8. Ratio of tertiary to quaternary, aromatic carbon in coke on the used catalysts A, B and C.

reactions involving coke precursors like asphaltenes. Asphaltenes, after precipitation on the catalyst surface, undergo dealkylation, dehydrogenetion and cyclization reactions on the acid sites and condense to high molecular weight polynuclear aromatics to form coke [6,24,30,32].

The data presented in Fig. 6 show that coke formed on CAT A and B was more aromatic (Car/C ≈ 0.7) than that formed on CAT C (Car/C = 0.4). Compared with the asphaltenes in KAR (AR/AS in Fig. 6), the coke deposits on both types of catalysts (A and B) were more aromatic, less substituted (σ = Car;alk/[Car;t + Car;alk] in Fig. 7) and less condensed (γ = [Car;b2 + Car;b3]/Car in Fig. 7). The deposits on catalyst C are not only less substituted and condensed, but also less aromatic than the asphaltenes in the atmospheric residue feed (AR/AS).

The aromaticity and other structural features of the carbonaceous deposits, such as the degree of condensation (γ) and alkyl-substitution (σ), depend largely on the hydrogenation and cracking functions of the catalyst. The CAT A (HDM) that contains unpromoted Mo on γ-alumina has low hydrogenation activity compared with the Ni-promoted CAT B (HDS) and the Ni-P-promoted CAT C (HDS/HDN). The crackability and dealkylation activity of all three catalysts is fairly high, consequently, the aromatic rings in the coke precursors were cracked and alkyl side chains were cleaved, as indicated by the drastic drop in the two parameters γ and σ compared with AR/AS (Fig. 7).

In summary, the catalysts tested combine different catalytic functions, namely, cracking, dealkylation and hydrogeneation functions. In case of CAT A (HDM) and CAT B (HDS) the cracking and dealkylation functions prevailed over the hydrogenation function. On the other hand for CAT C (HDS/HDN) the hydrogenation activity was dominating. On all three tested catalysts, as a result of dealkylation and cracking, quaternary, aromatic carbon had been hydrogenated to tertiary, aromatic carbon leading to an increase of the Car; t/Car;q ratio compared that one of the coke precursor AR/AS (Fig. 8).

Owing to the remarkable high hydrogenation activity of CAT C (HDS/HDN) not only quaternary, aromatic carbon was converted to tertiary, aromatic carbon but also aromatic rings in the coke precursors were hydrogeneted to nephthenic rings resulting in a decrease of all three parameters, Car/C, σ and γ compared to the asphaltenes in AR/AS.

DRIFT. The DRIFT spectra of the used ARDS catalysts are displayed in Figs. 9–13. In the region from 3500 cm^{-1} to 2750 cm^{-1}, a strong IR absorption was observed which was assigned to the O–H valence vibrations of adsorbed moisture and OH groups of the Al_2O_3 catalyst carrier [33]. On top of the

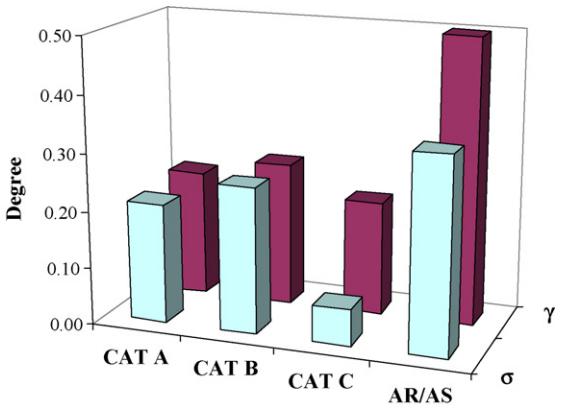

Fig. 7. Degree of alkyl-substitution (σ) and condensation (γ) in coke on the used catalysts A, B and C.

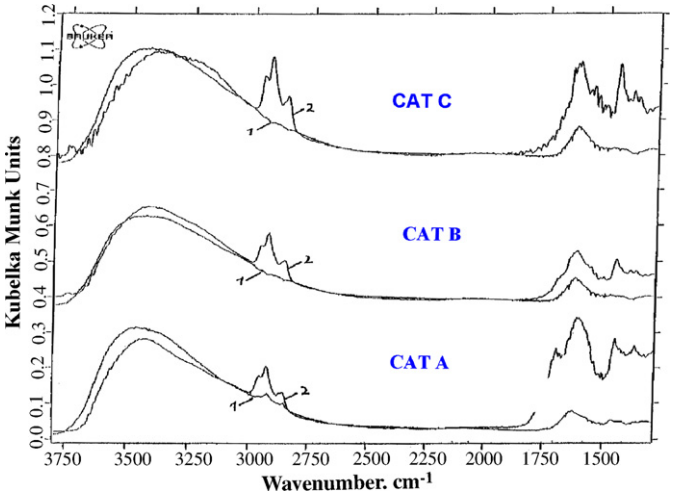

Fig. 9. DRIFT spectra of fresh (1) and used (2) catalysts A, B and C.

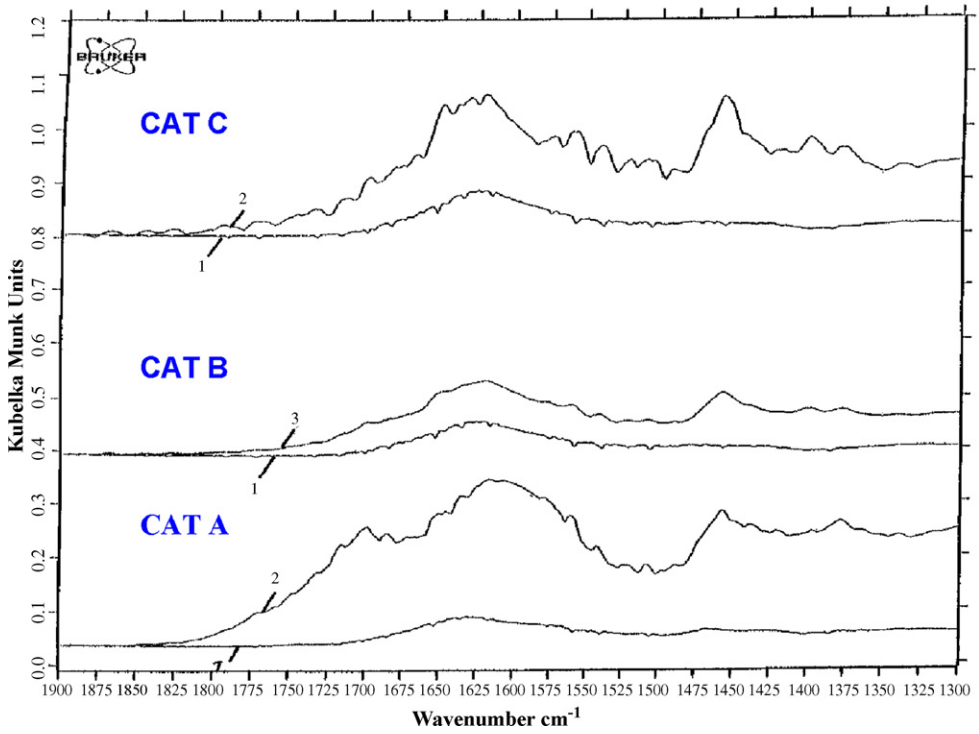

Fig. 10. DRIFT spectra of fresh (1) and used (2) catalysts A, B and C: carbonyl C=O (1750–1650 cm^{-1}); aromatic C=C (1630–1500 cm^{-1}) modes.

O–H band, aliphatic C–H bands of the asymmetric CH_2 and CH_3 stretching modes appeared at 2965 cm^{-1} and 2925 cm^{-1} [34,35]. The intensity of the aliphatic stretching bands can be mainly related to the amount of soft coke deposited.

In the carbonyl C=O (1750–1650 cm^{-1}) and the aromatic C=C (1630–1500 cm^{-1}) region, strong bands were observed, attributed to oxygen containing and conjugated polyaromatic structures, respectively. As seen in the spectra of the fresh catalysts (Figs. 9–11; traces No. 1), the O–H deformation modes at 1625 cm^{-1} of OH groups linked to the catalyst support also contributed to these IR bands in that region. Figs. 9–11, upper spectrum, show the FT-IR difference spectra of the used and fresh catalysts, respectively. Curve fitting revealed the presence of at least one IR band at about 1700 cm^{-1}, attributed to C=O stretching modes [33], best seen in the spectrum of used HDM catalyst (Fig. 9), one at about 1625 cm^{-1}, due to C=C in conjugated double bonds [36], and another one at about 1575 cm^{-1}, assigned as the so-called ''coke peak'' [25,33–35]. The ''coke peak'' is more prominent in the HDM (CAT A) and HDS/HDN (CAT C) catalysts than in the HDS catalyst. It is also seen in Fig. 9 that the coke peak at 1575 cm^{-1} for the HDM and HDS/HDN catalysts have similar intensities indicating that the difference in the amount of coke deposit in these two catalysts is not appreciably different. It is difficult to make a definite conclusion regarding the ranking of the two catalysts (CAT A or CAT C) for coke formation based on the DRIFT spectra results.

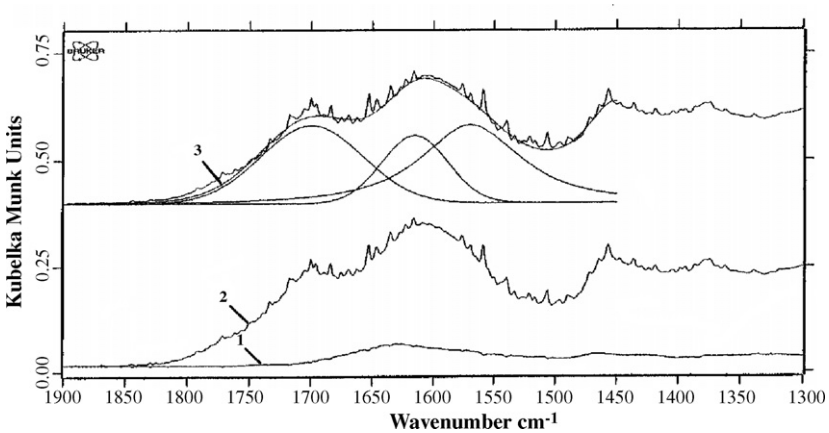

Fig. 11. Curve fitted DRIFT spectrum of carbonyl C=O (1750–1650 cm^{-1}) and aromatic C=C (1630–1500 cm^{-1}) modes of used CAT A: fresh (1), used (2) and fitted (3).

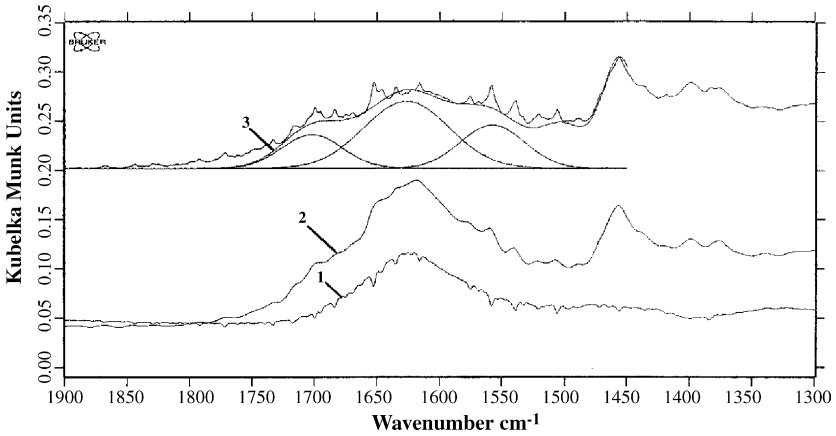

Fig. 12. Curve fitted DRIFT spectrum of carbonyl C═O (1750–1650 cm^{-1}) and aromatic C═C (1630–1500 cm^{-1}) modes of used CAT B: fresh (1), used (2) and fitted (3).

3.4. Metal deposition

Besides coke formation, metal deposition, especially of nickel and vanadium sulfides, is the second major deactivation route in hydrotreating of residua over ARDS catalysts containing nickel and molybdenum sulfides. The contribution of metal poisoning to the overall deactivation of ARDS catalysts is controversially reported. There is evidence that metal poisoning is negligible, at least during initial coking [37–39].

However, Gualda and Kasztelan [40] found, as they compared coke versus metal deactivation of a HDM Ni–Mo/Al_2O_3 catalyst (2.0 wt.% Ni, 8.4 wt.% Mo), that, in the early stages of the catalyst deactivation a small amount of V is more deactivating than a large amount of carbon. This result seems doubtful since coke deposition increases suddenly and rapidly right from the start of run [32,41,42] while metal poisoning is a steady and slow process which keeps the metal (V, Ni) content in the deposits at a low level during the start of the run phase [40,43].

Investigations in our laboratory on deactivation of a Mo/Al_2O_3 HDM catalyst (CAT A) by coking and metal deposition during hydrotreating of KAR [11] confirmed these findings. For instance, in contrast to carbon deposition which reached about 20 wt.% of fresh catalyst after 120 h, the amount of metals (V and Ni) deposited in the same period of time was only 2 wt.% (Fig. 14) [11]. Vanadium deposition on CAT A was, however, considerably higher than the nickel deposition. This is in line with the higher reactivity of vanadium-containing species present in the residual oil. However, towards the end of run, it is believed that deactivation by pore plugging by the metals (Ni and V) from the feed is the dominating path for catalyst decay [8,44].

Table 8 presents the amount of metals deposited after 120 h and physical properties of the three used ARDS catalysts examined in this study. The loss of surface area of the used catalysts compared with the fresh ones is attributed to a combination of coke and metal sulfide deposition. The strong reduction in surface area, pore volume and average pore diameter observed for CAT C (HDS/HDN) might be a result of extensive of blockage of the narrow pores by carbon and metal sulfide deposition.

Distribution profiles of metal on catalysts were examined by electron probe micro-analysis (EPMA). Generally, the extent of deactivation of residual oil hydrotreating catalysts by coke and metal depend, to a large extent, on the location of the deposits

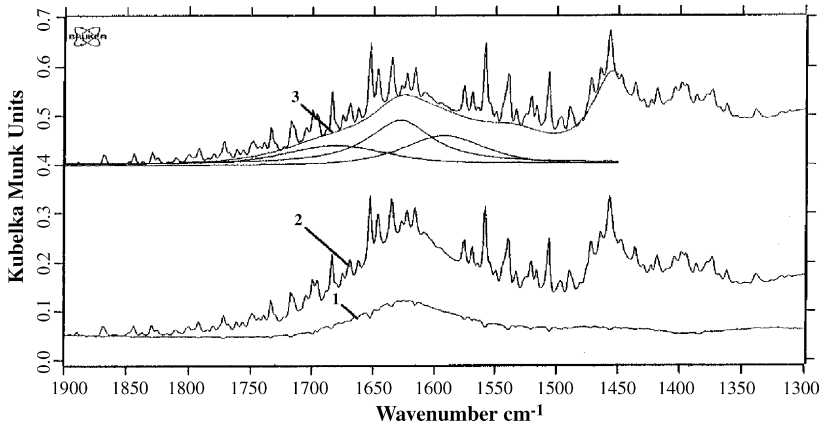

Fig. 13. Curve fitted DRIFT spectrum of carbonyl C═O (1750–1650 cm^{-1}) and aromatic C═C (1630–1500 cm^{-1}) modes of used CAT C: fresh (1), used (2) and fitted (3).

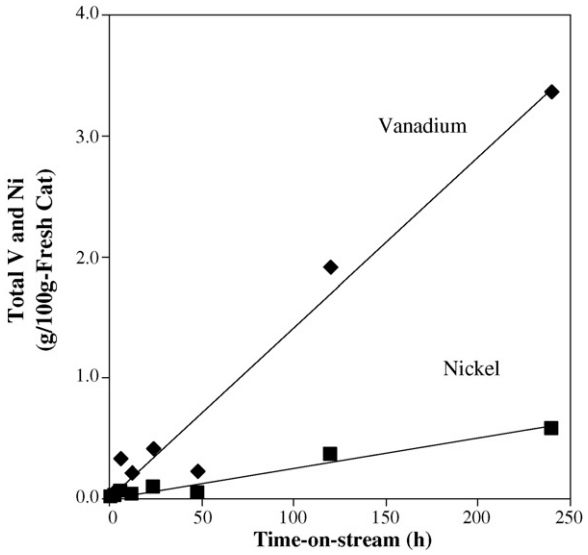

Fig. 14. Metal (V, Ni) deposition on the used CAT A (HDM) as a function of time-on-stream [11].

Table 8
Physical properties and metals deposition of three used industrial ARDS catalysts exposed to KAR for 120 h at 380 °C and LHSV 1 h^{-1}

Catalyst	Loss (%)			Deposited metals[a]	
	Surface area	Pore volume	Average pore diameter	V (wt.%)	Ni (wt.%)
CAT A	19	36	20	1.41	0.29
CAT B	29	42	28	1.13	0.49
CAT C	36	82	71	0.36	0.70

[a] Difference between metal concentration in feed and product oils.

within the catalyst pellet. If the deposits are concentrated near the outer edges, they can lead to pore mouth plugging and result in a rapid deactivation of the catalyst. On the other hand, a uniform distribution throughout the pellet's cross section will not reduce the catalyst's activity to a significant level.

The electron probe microanalyses of used ARDS catalysts are shown in Figs. 15 and 16. Vanadium which had the highest

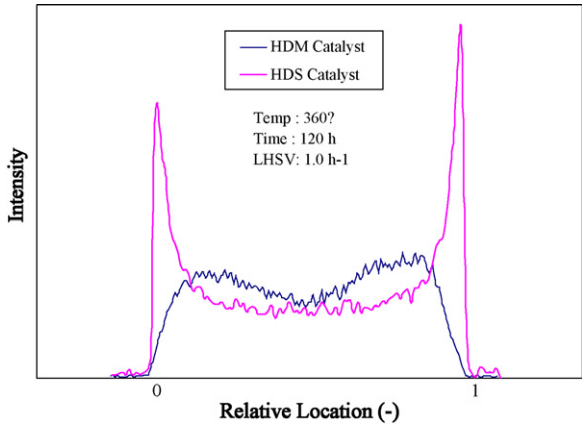

Fig. 15. Electron micro probe profile of vanadium distribution across the pellets of used CAT A (HDM) and CAT B (HDS) for the operating conditions: temperature, 380 °C; LHSV, 1.0 h^{-1}; time-on-stream, 120 h.

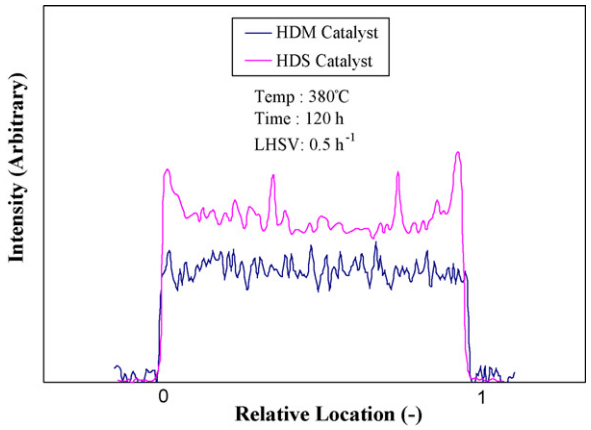

Fig. 16. Electron micro probe profile of nickel distribution across the pellets of used CAT A (HDM) and CAT B (HDS) for the operating conditions: temperature, 380 °C; LHSV, 1.0 h^{-1}; time-on-stream, 120 h.

concentration on the used CAT A (HDM), was almost uniformly distributed throughout the pellet (Fig. 15). On the narrow pore CAT B (HDS), vanadium was preferentially localized near the pellet edges (Fig. 15). Diffusion limitation and high reactivity of the vanadium-carrying molecules in the feed might have induced this vanadium radial concentration gradient. The concentration of V on the used CAT C (HDS/HDN) was too low to measure a profile.

In contrast to the vanadium distribution, nickel was nearly uniformly distributed across the pellets of the three types of catalysts, as the EPMA data indicated (Fig. 16). Only on used CAT A (HDM), the added Ni increased slightly towards the edges. The profiles in Figs. 15 and 16 were obtained from three randomly chosen pellets, and statistically justified results need a larger variety of samples to be analyzed.

4. Conclusions

Catalyst deactivation is a serious problem in residual oil hydrotreating. It may occur through complex processes that are affected by several factors, such as catalyst type, operating conditions, feedstock properties and reactor design. In the present work, as part of a joint research project between Japan Co-operation Center, Petroleum, Japan, and KISR to study the deactivation behavior of hydrotreating catalysts used in KNPC's ARDS processes, performance tests were conducted on three types of hydrotreating catalysts, namely, a Mo/Al_2O_3 (HDM), a $Ni–Mo/Al_2O_3$ (HDS), and a $Ni–Mo/Al_2O_3$ (HDS/HDN) catalyst, that have been used in the reactor train of KNPC's ARDS units. Three experiments were carried out with Kuwait atmospheric residue under similar operating conditions: time-on-stream; 120 h, T; 380 °C, LHSV; 1 h^{-1}, p; 120 bar and H_2/Oil ratio; 570. The used catalysts from these experiments were fully characterized by chemical analysis and various advanced analytical techniques, such as solid-state ^{13}C NMR TPO, EPMA and IR. The following are the important results and conclusions of the study.

The results indicated that the coke build-up during the initial phase of hydrotreating was very fast and the amount of carbon

deposited reached about 20 wt.% of the fresh catalyst within 120 h. The tendency of coking increased in the sequence: HDS < HDM < HDS/HDN. TPO analysis showed two types of coke, namely, soft coke and refractory surface coke, on the spent catalysts. NMR data indicated that coke deposits on the HDM and HDS catalysts were more aromatic and more condensed with less alkyl substituents compared to the HDS/HDN catalyst. The coke was exclusively adsorbed at the catalyst support, and the active metal sulfide phase was free from coke. The surface coke contained heteroatoms such as sulfur and nitrogen. These heteroatoms were, however, not present in the soft coke. Nitrogen compounds were also found strongly adsorbed on the active metal sulfide sites. Depending on the type of catalyst, the coke exhibited differences in it's structure. The HDS/HDN catalyst had high hydrogenation activity which led to a highly saturated coke with aromaticity even lower than that of the asphaltenic coke precursors in the atmospheric residue feed. DRIFT spectroscopy confirmed coking tendency of the three tested catalysts. Regarding the distribution of deposited vanadium across the catalyst pellet, the three types of catalysts fell into two groups. The HDM catalyst showed a nearly uniform distribution. On the other two catalysts that had narrow pores HDS catalyst, vanadium was preferentially localized near the pellet edges. In all three tested catalysts, nickel was uniformly distributed. The loss in catalyst surface area and pore volume was substantial during the early stages of the run. The HDS/HDN catalyst suffered higher losses in surface area than other two catalysts. The results clearly show that the physico–chemical properties of the catalysts have a strong influence on catalyst deactivation by coke and metal deposition.

Acknowledgements

This work is a joint project between Japan Co-operation Center, Petroleum (JCCP) funded by the Ministry of Economic, Trade and Industry (METI), Japan and Kuwait Institute for Scientific Research (KISR), Kuwait. It bears the KISR Project No. PF010C.

References

[1] A. Al-Nasser, S.R. Chaudhuri, S. Bhattacharya, Stud. Surf. Sci. Catal. 100 (1996) 171–180.
[2] T.M. Saleh, H. Ismail, J.E. Corbett, R.S. Bali, Stud. Surf. Sci. Catal. 53 (1990) 175–189.
[3] A. Abbas, S.R. Chaudhuri, S. Battacharya, in: Proceedings of the Eighth Annual Saudi–Japanese Symposium, The Research Institute, King Fahad University for Petroleum and Minerals, Dahran, Saudi Arabia, November, (1998), p. 175.
[4] E. Furimsky, Appl. Catal. A: Gen. 171 (1998) 177.
[5] C.T. Adams, A.A. Del Peggio, H. Schaper, W.H.J. Stork, W.K. Shiflett, Hydrocarb. Process (1989) 57.
[6] M. Absi-Halabi, A. Stanislaus, D.L. Trimm, Coke formation on catalysts during the hydroprocessing of heavy oil, Appl. Catal. 72 (1991) 193–215.
[7] C.H. Bartholomew, in: M. Oballa, S.S. Shih (Eds.), Catalytic Hydroprocessing of Petroleum and Distillates, Marcel Dekker, New York, 1994 , p. 1.
[8] E. Furimsky, F.E. Massoth, Catal. Today 52 (1999) (1999) 381.
[9] K. Al-Dalama, A. Stanislaus, Chem. Eng. J. 120 (2006) 33.
[10] P. Hannerup, A.C. Jacobsen, ACS Petrol. Chem. Div. (1983) 576, Preprints 28.
[11] K. Matsushita, A. Hauser, A. Marafi, A. Stanislaus, Fuel 83 (2004) 1031.
[12] A. Hauser, A. Al-Adwani, A. Stanislaus, A. Marafi, K. Matsushita, Fuel 84 (2005) 259.
[13] A. Marafi, H. Al-Bazzazi, M. Al-Marri, F. Maruyama, M. Absi-Halabi, A. Stanislaus, Energy Fuels 17 (2003) 1191.
[14] A. Hauser, A. Marafi, A. Stanislaus, A. Al-Adwani, Energy Fuels 19 (2005) 544.
[15] A. Stanislaus, M. Absi-Halabi, K. Al-Dolama, Appl. Catal. 39 (1988) 239.
[16] M. Absi-Halabi, A. Stanislaus, T. Al-Mghni, S. Khan, A. Qamra, Fuel 74 (1995) 1211.
[17] H. Beuther, O.H. Larson, A.J. Perrotta, Stud. Surf. Sci. Catal. 6 (1980) 271.
[18] I. Mochida, Y.Z. Zhoa, K. Sakanishi, S.I. Yamamoto, H.A. Tokashima, S.J. Vemura, Ind. Eng. Chem. Res. 28 (1989) 418.
[19] S.M. Augustine, G.N. Alameddin, W.M.H. Sachtler, J. Catal. 155 (1989) 217.
[20] P. Zeuthen, H. Cooper, F.T. Clark, D. Arter, Ind. Eng. Chem. Res. 34 (1995) 755.
[21] P. Zeuthen, P. Blom, F.E. Massoth, Appl. Catal. 78 (1991) 265.
[22] M. Behbehani, A. Hauser, F. Ali, H. Abdullah, Petrol. Sci. Technol. 17 (1999) 1011.
[23] Y.M. Zhorov, L.A. Ostrer, Chem. Tech. Fuels Oil 26 (1991) 226.
[24] E. Furimsky, F.E. Massoth, Catal. Today 17 (1993) 537.
[25] C. Li, Y.W. Chen, S.J. Yang, R.B. Yen, Appl. Surf. Sci. 81 (1994) 465.
[26] P. Dufresne, ACS Petrol. Chem. Div. 38 (1993) 54, Preprints.
[27] Y. Yoshimura, E. Furimsky, T. Sato, H. Shimada, N. Matsubayashi, A. Nishijima, in: Proceedings of the Ninth International Congress on Catalysis Calargy, vol. 1, 1988, pp. 136–143.
[28] E. Furimsky, Erdöl Kohle 35 (1982) 455.
[29] P. Zeuthen, P. Blom, B. Muegge, F.E. Massoth, Appl. Catal. 68 (1991) 117.
[30] S.M. Richardson, H. Nagaishi, M.R. Gray, Ind. Eng. Chem. Res. 35 (1996) 3940.
[31] J. Van Doorn, J.A. Moulijn, Catal. Today 7 (1990) 257.
[32] A. Stanislaus, A. Hauser, A. Marafi, Catal. Today 109 (2005) 167.
[33] J.V. Ibarra, C. Royo, A. Monzón, J. Santamaria, Vib. Spectrosc. 9 (1995) 191.
[34] D.G. Blackmond, F.G. Goodwin, J. Catal. 78 (1982) 34.
[35] D. Eisenbach, E. Gallei, J. Catal. 56 (1979) 377.
[36] A.G. Gayubo, J.M. Arandes, A. Aguayo, M. Olazar, J. Bilbao, Ind. Eng. Chem. Res. 32 (1993) 588.
[37] M. Yumoto, S.G. Kukes, M.T. Klein, B.C. Gates, Catal. Lett. 26 (1994) 1.
[38] M. Yumoto, S.G. Kukes, M.T. Klein, B.C. Gates, Ind. Eng. Chem. Res. 35 (1996) 3203.
[39] M. Yumoto, S.G. Kukes, M.T. Klein, B.C. Gates, Ind. Eng. Chem. Res. 41 (2001) 131.
[40] G. Gualda, S. Kasztelan, Stud. Surf. Sci. Catal. 88 (1994) 145.
[41] A. Nishijima, H. Shimada, Y. Yoshimura, T. Sato, N. Matsubayashi, Stud. Surf. Sci. Catal. 34 (1987) 39.
[42] P. Zeuthen, J. Bartholdy, P. Wiwel, B.H. Cooper, Stud. Surf. Sci. Catal. 88 (1994) 199.
[43] L. Reyes, C. Zerpa, J.H. Krasuk, Stud. Surf. Sci. Catal. 88 (1994) 85.
[44] R.J. Quan, R.A. Ware, C.W. Hung, J. Wei, Adv. Chem. Eng. 14 (1988) 95.